

# **Halogenated Volatile Additive Strategy for Regulating Crystallization Kinetics and Enabling 20.40% Efficiency Polymer Solar Cells with Low Non-Radiative Recombination Energy Loss**

*Changjiang Li, Min Deng,\* Haonan Chen, Yuwei Duan, Chentong Liao, Zeqin Chen\* and Qiang Peng\**

C. J. Li, Dr. M. Deng, H. N. Chen, Dr. Y. W. Duan, Dr. C. T. Liao, Prof. Z. Q. Chen, Prof. Q. Peng

College of Materials and Chemistry & Chemical Engineering, Chengdu University of Technology,  
Chengdu 610059, P. R. China

E-mail: [mindeng@cdut.edu.cn](mailto:mindeng@cdut.edu.cn); [chenzeqin19@cdut.edu.cn](mailto:chenzeqin19@cdut.edu.cn); [qiangpeng@scu.edu.cn](mailto:qiangpeng@scu.edu.cn)

Prof. Q. Peng

School of Chemical Engineering and State Key Laboratory of Polymer Materials Engineering, Sichuan  
University, Chengdu 610065, P. R. China

E-mail: [qiangpeng@scu.edu.cn](mailto:qiangpeng@scu.edu.cn)

## 1. Materials and Methods

**Materials:** PM6 and L8-BO were purchased from Solarmer Material Inc. 1-fluoro-3,5-dimethoxybenzene (F-DMB), 1-chloro-3,5-dimethoxybenzene (Cl-DMB), 1-bromo-3,5-dimethoxybenzene (Br-DMB), 1-iodo-3,5-dimethoxybenzene (I-DMB) and (4-(3,6-diphenyl-9H-carbazol-9-yl)butyl)phosphonic (Ph-4PACz) were purchased from Tansoole. All the other chemicals were purchased from Aladdin, Adamas, Sigma-Aldrich and Alfa Aesar Chemical Co., and used without further purification. All solvents were freshly distilled immediately prior to use.

## 2. Material characterizations

Thermogravimetric analysis (TGA) was conducted on a TA Instrument Model SDT Q600. Surface energies were measured using a KRÜSS DSA100 drop shape analyzer with water and diiodomethane as testing liquids. UV-vis spectra were obtained on a Hitachi U2910 spectrophotometer. Femtosecond transient absorption spectroscopy (fs-TAS) was conducted using a commercial Helios setup from Ultrafast Systems with a Ti:sapphire regenerative amplified laser system (Coherent Libra) delivered laser pulses at 780 nm (100 fs, 1 kHz). An optical parametric amplifier (Vitara, Coherent) pumped by the regenerative amplifier was used to generate the pump beam at 630 nm (at wavelength resonant with the absorption of PM6). The probe beam was generated by focusing part of the fundamental femtosecond laser beam onto a sapphire plate or Yttrium aluminum garnet plate for visible (vis) and near-IR (NIR) spectral windows, respectively. TA results in this work are presented in the unit of  $\Delta OD$ , negative features can reflect ground-state bleaching (GSB) or stimulated emission

(SE), a positive signal is an excited-state absorption (ESA). During TA measurements, the samples were kept in nitrogen to avoid photodegradation. The pump fluence was kept at  $<5 \mu\text{J cm}^{-2}$  to minimize the exciton-exciton annihilation effect. GIWAXS measurements were performed on a Xenocs X-ray Small-angle Scatterer (Xeuss 2.0) with the Pilatus 3R 300K detector. AFM images were obtained by using a Bruker Nano IR3 atomic microscope in tapping mode. The Fourier-transform infrared spectroscopy (FTIR) spectra (KBr) were recorded on a Bruker Tensor 27 Infrared spectroscope in transmission mode. FTIR data were reported with a wavenumber ( $\text{cm}^{-1}$ ) scale. The PiFM images were collected on a Bruker NanoIR-3 atomic force microscope in contact mode.

### **3. Fabrication and characterization of polymer solar cells**

#### **3.1 Fabrication of polymer solar cells devices**

(1) Cleaning of indium tin oxide (ITO) conductive glass: Clean the glass with detergent, deionized water, ethanol and acetone. Then dry and clean the ITO conductive glass with high-purity nitrogen gas to ensure that there is no liquid residue on the surface. Finally, treat the surface with ultraviolet ozone for 20 min to further purify the surface and enhance its adhesion. (2) Preparation of Ph-4PACz: Accurately weigh Ph-4PACz, dissolve it in anhydrous ethanol at a concentration of  $0.3 \text{ mg mL}^{-1}$ , sonicate for 30 min, and stir at  $40 \text{ }^\circ\text{C}$  for 6 h. (3) Preparation of active layer solution: Accurately weigh PM6 and L8-BO with a mass ratio of 1:1.2. Dissolve PM6 and L8-BO in chloroform solution and strictly control the concentration of PM6 at  $8 \text{ mg mL}^{-1}$ . Add 0.6% (v/v) F-DMB and 60% (w/w) Cl-DMB, Br-DMB and I-DMB into the active layer solution. Stir at room temperature for 1.5 h to ensure

complete dissolution. (4) Preparation of PNDIT-F3N: Accurately weigh PNDIT-F3N and dissolve it in a mixed solvent of methanol and glacial acetic acid (v/v = 200:1), strictly controlling the concentration at  $0.8 \text{ mg mL}^{-1}$ . Stir at room temperature for 30 min to ensure complete dissolution. (5) Preparation of device: Spin coat Ph-4PACz solution onto the surface of ITO glass at a speed of 3000 rpm, and annealed at  $80 \text{ }^\circ\text{C}$  for 5 min to form the hole transport layer ( $\sim 15 \text{ nm}$ ). Then, spin coat the active layer solution onto ITO/Ph-4PACz at the same speed and annealed at  $90 \text{ }^\circ\text{C}$  for 10 min to obtain active layer with thickness of approximately 100 nm. Spin coat PNDIT-F3N solution onto the active layer to construct the electron transport layer ( $\sim 5 \text{ nm}$ ). Finally, the standardized device with effective area of  $4.00 \text{ mm}^2$  and thickness of 90 nm silver electrode was obtained by evaporating silver in high vacuum chamber of  $1 \times 10^{-5} \text{ Pa}$ . To improve our manuscript, we supplemented the sample preparation process in detail in the supporting information.

### **3.2 Fabrication of hole-only and electron-only devices**

Hole-only and electron-only devices for SCLC measurements were fabricated with similar methods in architectures of ITO/PEDOT:PSS/active layer/Au and ITO/ZnO/active layer/PNDIT-F3N/Ag, respectively. The ZnO layer was fabricated using a sol-gel method, and gold electrodes were deposited by thermal evaporation in vacuum. All device fabrications were performed in an argon gas filled glove box except for the deposition of PEDOT:PSS and ZnO layers.

### **3.3 Device measurements**

The  $J$ - $V$  characteristics of devices were recorded using a Keithley 2400 Source Measure Unit

under AM1.5 G (100 mW cm<sup>-2</sup>) irradiation generated by a SAN-EI XES-70S1 solar simulator in an argon gas filled glove box. The EQE responses from PSC devices were recorded on an Enlitech QE-R solar quantum efficiency testing system in air. PSC devices for EQE, charge generation and charge recombination evaluations were the top performing devices. Charge carrier mobilities were tested using the space charge limited current (SCLC) method on hole-only and electron-only devices. The  $J$ - $V$  curves measured on hole-only and electron-only devices were fitted to  $J = 9\epsilon_0\epsilon_r\mu V^2/8L^3$ , where  $J$  is the current density,  $L$  is the film thickness of the active layer,  $\mu$  is the hole or electron mobility,  $\epsilon_r$  is the relative dielectric constant of the transport medium,  $\epsilon_0$  is the permittivity of free space ( $8.85\times 10^{-12}$  F m<sup>-1</sup>),  $V$  is the internal voltage in the device and  $V = V_{\text{appl}} - V_{\text{bi}} - V_{\text{a}}$ , where  $V_{\text{appl}}$  is the applied voltage to the device,  $V_{\text{bi}}$  is the built-in voltage and  $V_{\text{a}}$  is the voltage drop. Transient photovoltage (TPV), transient photocurrent (TPC) and photogenerated charge extraction by linearly increasing voltage (photo-CELIV) mobilities data were obtained by the all-in-one characterization platform, Paios (Fluxim AG, Switzerland). In the TPV measurement, the settling time was 10 ms, pulse length was 10  $\mu$ s and the follow-up time was 500  $\mu$ s. In the TPC measurement, the settling time was 5  $\mu$ s, pulse length was 5  $\mu$ s and the follow-up time was 50  $\mu$ s. In the photo-CELIV measurement, the delay time was set to 0  $\mu$ s, the light intensity was 100%, the light-pulse length was 100  $\mu$ s, finally the sweep ramp rate rose from 20 V ms<sup>-1</sup> to 100 V ms<sup>-1</sup>.  $EQE_{\text{EL}}$  values were obtained from an in-house-built system including a Hamamatsu silicon photodiode 1010B, a Keithley 2400 SourceMeter to provide voltage and inject current, and a Keithley 6482 Picoammeter to measure the emitted light intensity. Highly sensitive EQE

(sEQE) measurements were performed using a halogen lamp, a monochromator (Newport cornerstone cs260), an optical chopper, a pre current amplifier (Stanford Instrument SR-570), a lock-in amplifier (Stanford Instrument SR 830), and a set of long pass filters.

#### 4. Supporting Figures

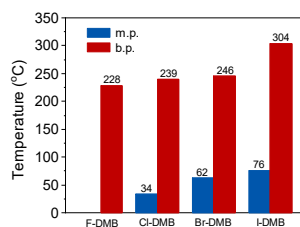


**Fig. S1** Histogram of m.p. and b.p. of halogenated volatile additives.

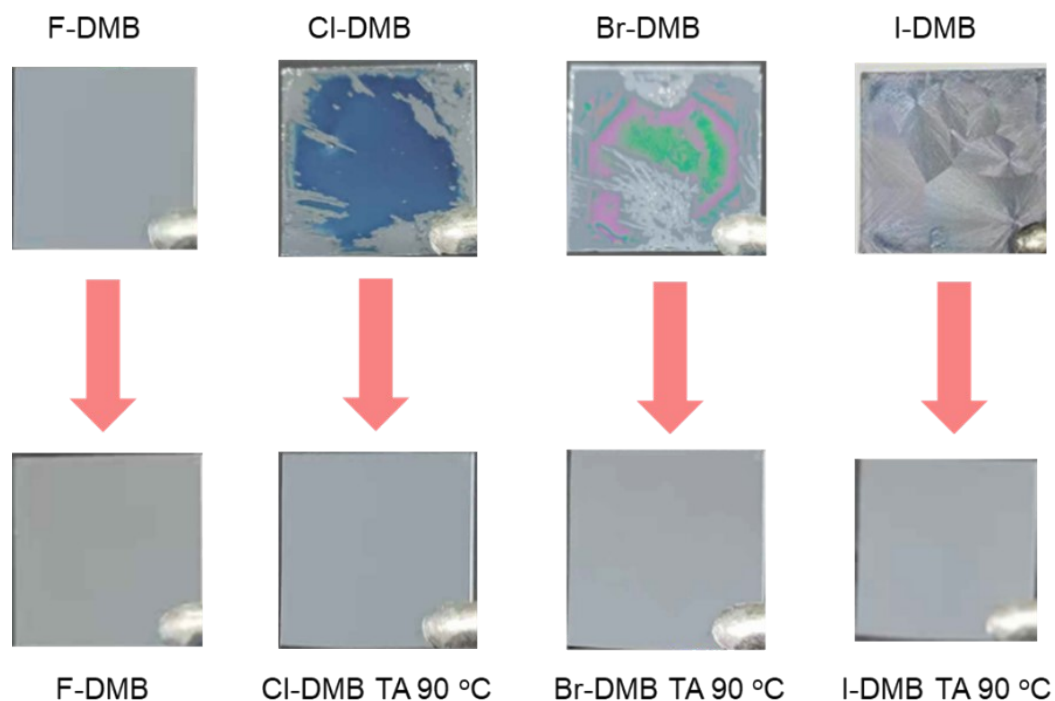


**Fig. S2** Images of spin coating chloroform solution with additive ( $12 \text{ mg mL}^{-1}$ , spin coating speed of 3000 r.p.m.) on silicon wafer without (up) and with thermal annealing (down) treatment.

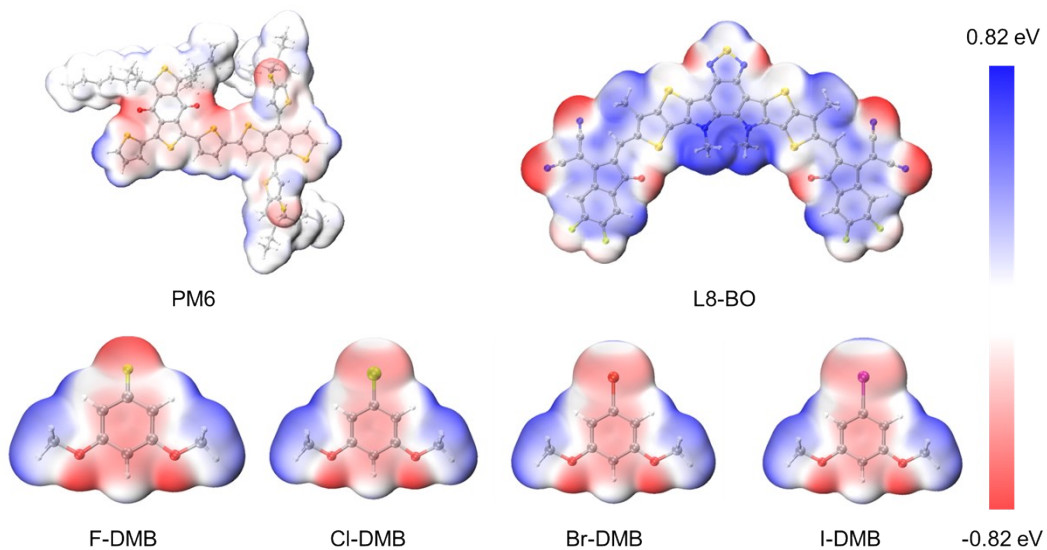


**Fig. S3** ESP distribution of PM6, L8-BO and halogenated volatile additives.

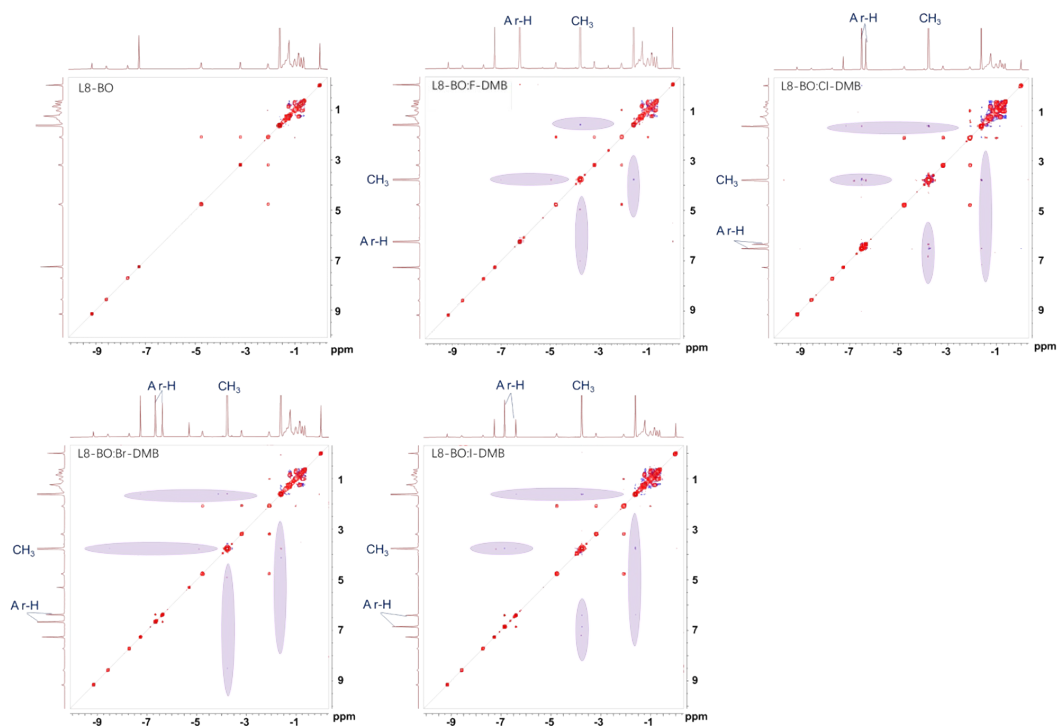


**Fig. S4** The 2D-NMR NOESY spectra of L8-BO and that containing additive. The marked Ar-H and CH<sub>3</sub> denoted the <sup>1</sup>H resonance peaks from the benzene cores and the methyl groups of these additives,

respectively. The crossover resonance signals between the additives and L8-BO were marked with light purple.

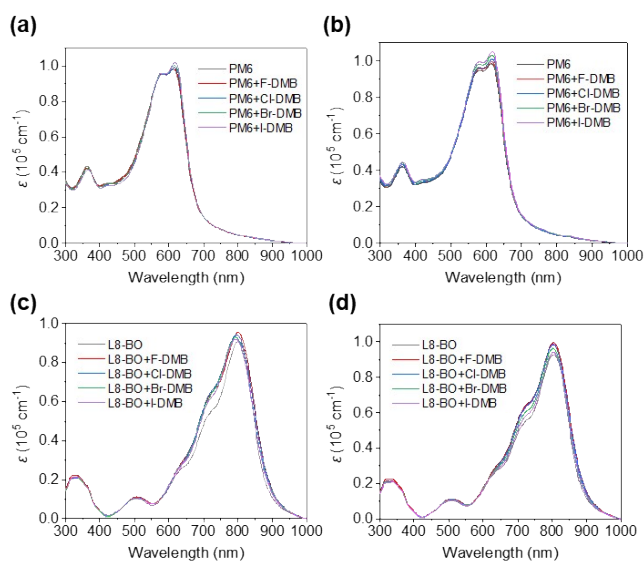


**Fig. S5** UV-vis-NIR absorption spectra of PM6 and L8-BO without and with additives in solid-state films before (a, c) and after (b, d) thermal annealing.

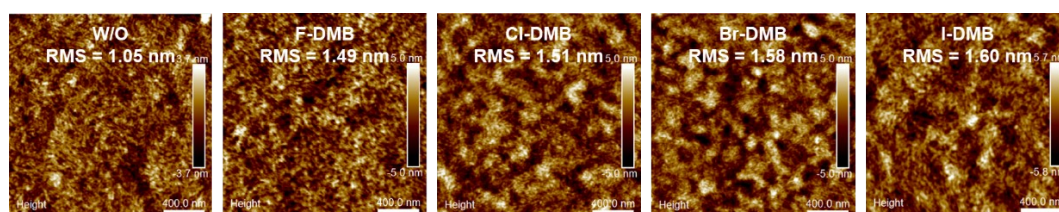


**Fig. S6** AFM height images of PM6 and PM6 containing additives.

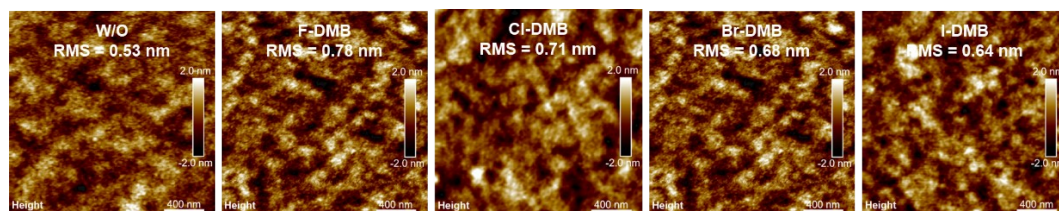


**Fig. S7** AFM height images of L8-BO and L8-BO containing additives.

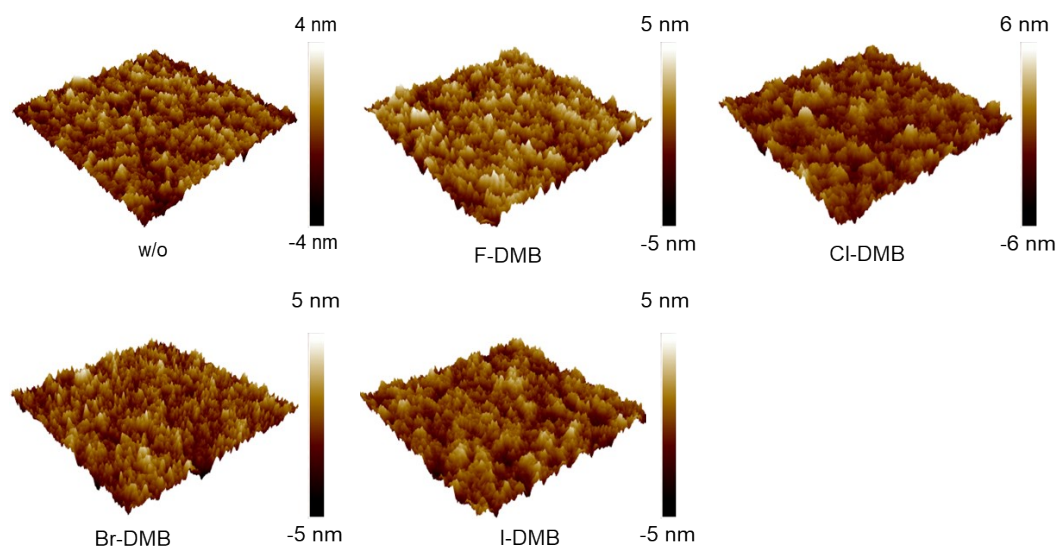


**Fig. S8** 3D AFM height images of blend films.

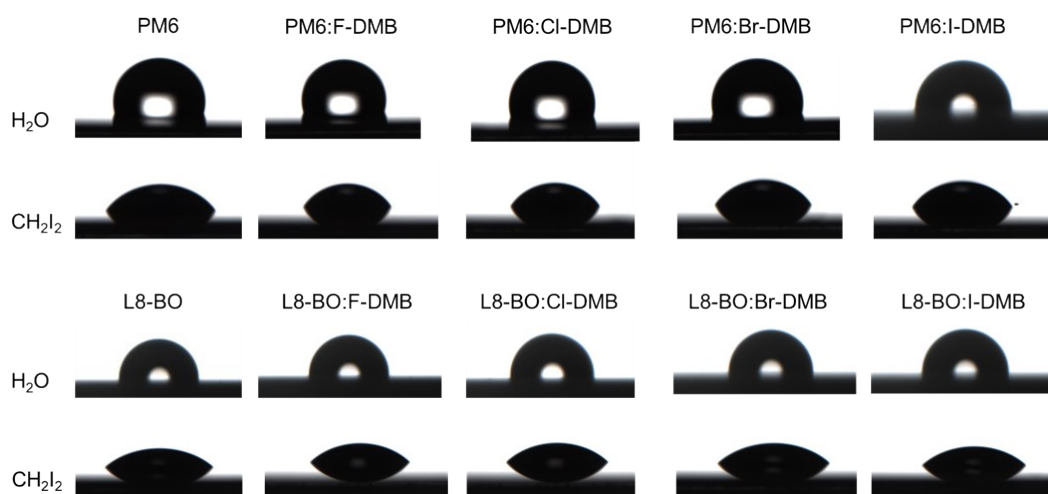


**Fig. S9** Surface energy measurements of photovoltaic materials used in this work.

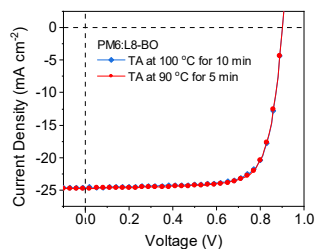


**Fig. S10**  $J$ - $V$  curves of the PM6:L8-BO devices processed with different post-processing methods.

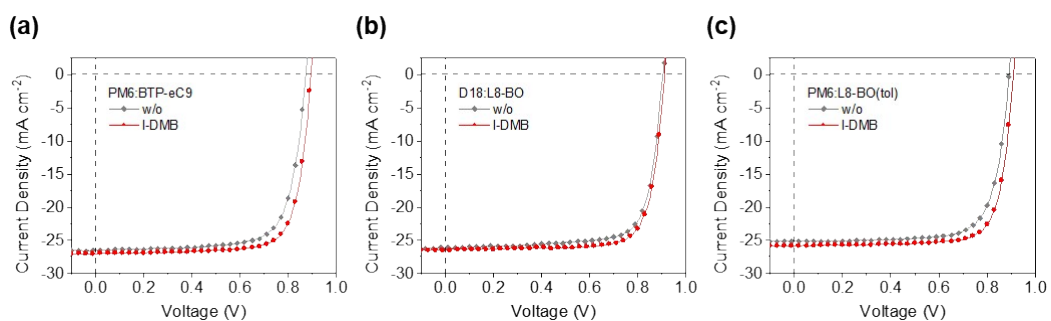


**Fig. S11** (a, b)  $J$ - $V$  curves of the PM6:BTP-eC9 (a), D18:L8-BO (b) devices and those containing additive I-DMB. (c)  $J$ - $V$  curves of the PM6:L8-BO devices processed with toluene.

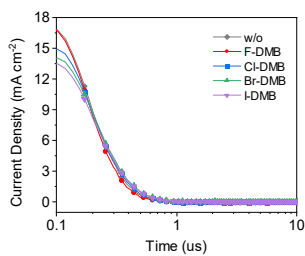


**Fig. S12** DLTS curves of PM6:L8-BO without and with additives.

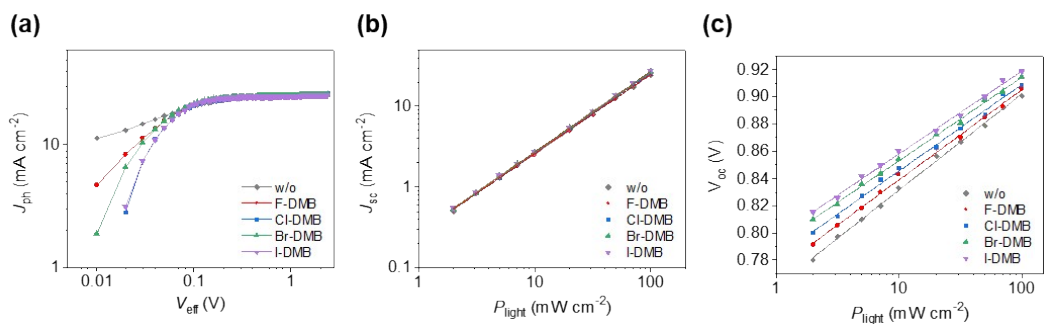


**Fig. S13** (a) Photocurrent versus the effective voltage of the PSCs. (b)  $J_{sc}$  and (c)  $V_{oc}$  versus  $P_{light}$  plots of the PSCs.

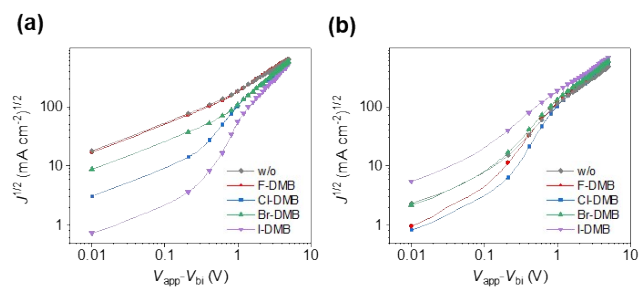


**Fig. S14** (a) Hole mobilities and (b) electron mobilities of PSCs.

**Table S1** Parameters of contact angles and surface energies of films.

| additive | film  | contact angle (°) |                                | surface energy<br>(mJ m <sup>-2</sup> ) | $\chi$ |
|----------|-------|-------------------|--------------------------------|---|--------|
|          |       | H <sub>2</sub> O  | CH <sub>2</sub> I <sub>2</sub> |   |        |
| w/o      | PM6   | 103.62            | 52.34                          | 32.97                                   | 0.39   |
|          | L8-BO | 90.00             | 39.94                          | 40.60                                   |        |
| F-DMB    | PM6   | 105.24            | 57.35                          | 30.13                                   | 0.68   |
|          | L8-BO | 91.39             | 41.11                          | 39.83                                   |        |
| Cl-DMB   | PM6   | 104.50            | 56.16                          | 30.81                                   | 0.64   |
|          | L8-BO | 93.24             | 39.33                          | 40.40                                   |        |
| Br-DMB   | PM6   | 102.78            | 56.29                          | 30.62                                   | 0.58   |
|          | L8-BO | 94.87             | 40.46                          | 39.63                                   |        |
| I-DMB    | PM6   | 104.54            | 55.28                          | 31.31                                   | 0.51   |
|          | L8-BO | 96.41             | 39.94                          | 39.80                                   |        |

**Table S2** Summarized parameters for the ordered structures.

|        | Lamellar stacking   |      |                     |      | $\pi$ - $\pi$ stacking |      |
|--------|---------------------|------|---------------------|------|------------------------|------|
|        | q                   | d    | FWHM                | CCL  | q                      | d    |
|        | (nm <sup>-1</sup> ) | (nm) | (nm <sup>-1</sup> ) | (nm) | (nm <sup>-1</sup> )    | (nm) |
| w/o    | 3.11                | 2.02 | 0.85                | 6.58 | 17.66                  | 0.36 |
| F-DMB  | 3.08                | 2.04 | 0.59                | 9.48 | 17.50                  | 0.36 |
| Cl-DMB | 3.07                | 2.05 | 0.67                | 8.34 | 17.43                  | 0.36 |
| Br-DMB | 3.05                | 2.06 | 0.68                | 8.22 | 17.21                  | 0.36 |
| I-DMB  | 3.03                | 2.07 | 0.71                | 7.88 | 17.17                  | 0.37 |

**Table S3** Photovoltaic parameters of different post-processing methods of PM6:L8-BO devices.

| post-processing methods | $V_{oc}$<br>(V) | $J_{sc}$<br>(mA cm <sup>-2</sup> ) | FF<br>(%) | PCE<br>(%) |
|-------------------------|-----------------|------------------------------------|-----------|------------|
| TA at 100 °C for 10 min | 0.901           | 24.58                              | 75.82%    | 16.79      |
| TA at 90 °C for 5 min   | 0.901           | 24.73                              | 76.28     | 17.00      |

**Table S4** Photovoltaic parameters of the PM6:BTP-eC9 devices with/without I-DMB.

| active layer           | $V_{oc}$<br>(V) | $J_{sc}$<br>(mA cm <sup>-2</sup> ) | FF<br>(%) | PCE<br>(%) |
|------------------------|-----------------|------------------------------------|-----------|------------|
| PM6:BTP-eC9            | 0.872           | 26.55                              | 74.31     | 17.20      |
| PM6:BTP-eC9<br>(I-DMB) | 0.895           | 26.98                              | 77.22     | 18.65      |

**Table S5** Photovoltaic parameters of the D18:L8-BO devices with/without I-DMB.

| active layer         | $V_{oc}$<br>(V) | $J_{sc}$<br>(mA cm <sup>-2</sup> ) | FF<br>(%) | PCE<br>(%) |
|----------------------|-----------------|------------------------------------|-----------|------------|
| D18:L8-BO            | 0.905           | 26.12                              | 76.00     | 17.97      |
| D18:L8-BO<br>(I-DMB) | 0.912           | 26.46                              | 77.83     | 18.78      |

**Table S6** Photovoltaic parameters of the devices processed with toluene.

| active layer         | $V_{oc}$<br>(V) | $J_{sc}$<br>(mA cm <sup>-2</sup> ) | FF<br>(%) | PCE<br>(%) |
|----------------------|-----------------|------------------------------------|-----------|------------|
| PM6:L8-BO            | 0.890           | 25.11                              | 75.23     | 16.81      |
| PM6:L8-BO<br>(I-DMB) | 0.908           | 25.77                              | 78.22     | 18.30      |